Third generation rainfall climatologies: satellite rainfall and topography provide a basis for smart interpolation

Chris Funk[1], Greg Husak[1], Joel Michaelsen[1], Tim Love[2], and Diego Pedreros[1]

1. Climate Hazards Group, Department of Geography,
   University of California Santa Barbara, California
   Email: chris@geog.ucsb.edu

2. NOAA Climate Prediction Center
   Camp Springs, MD

Abstract

This short paper discusses a technique for producing 'improved rainfall estimates' (IRE) for Africa. The central objective of IRE is to make reasonable use of the high resolution mean fields, moderate density gauge data, and timely satellite rainfall data typically available at the national/regional level in Africa. In general, traditional rainfall interpolation schemes can be classified into two coarse categories. In the beginning, raw station observations were interpolated by combining the values of surrounding stations. Later, 2nd generation techniques interpolated anomalies from long terms means, thereby reducing the bias and error of the resulting estimates. For air temperature, the systematic relationship between elevation and station observations has been used as a basis for 'smart' interpolation, enhancing estimation accuracies even further. The relationship between precipitation and topography is, alas, substantially more complicated. This talks demonstrates how a combination of temporally-static 0.1 degree satellite-enhanced precipitation mean fields and coarse (2.5 degree) time-varying precipitation fields can be combined to provide a reasonable basis for the 'smart' interpolation of rainfall in areas of complex terrain and limited in situ gauge data. Accuracy assessments are carried out for Ethiopia and Kenya.

1.0 Introduction

In general, there have been two traditional approaches to producing gridded maps of meteorological variables. The first 'naïve' stage used various interpolation schemes to create spatially continuous grids from raw point data. This approach is highly dependent on the spatial distribution of gauges observations, and from the perspective of geo-statistics the non-stationarity of the background mean field violates the optimality constraints of kriging. For temperature fields, it was recognized that background mean fields, often related to elevation via lapse rate relationships, could be estimated and used to provide dramatic enhancements in accuracy. While some success in producing similar advances in precipitation have been achieved, this type of background-augmented 'smart' interpolation of precipitation has proven difficult to achieve in data-sparse Africa. In this paper we discuss how new satellite-based precipitation fields may be blended with traditional 2nd generation rainfall gridding procedures to produce 3rd generation precipitation climatologies that have several desirable characteristics: low bias, high fidelity, near-climatological period of record, and reasonable latency periods.

2.0 Data

Three data sources were combined to produce satellite enhanced mean fields: long term (1996-2005) monthly means derived from the Climate Prediction Center African Rainfall Climatology (ARC, Love et al., 2004), USGS Hydro 1K (Gesch et al., 1999) slopes and elevation data resampled to the ARC 0.1° grid, and FAO climate normals. We demonstrate the method with two sets of satellite rainfall estimates: the 27 year Global Precipitation Climatology Project data (GPCP, Huffman et al., 1995, 1997, Adler et al., 2003) and the 10 year ARC over Africa. Time-series of station data were obtained by combining data from the Global Historical Climate Network (Peterson and Vose, 1997), FAOCLIM2.0 (FAO, 2001) with data obtained from the Ethiopian Meteorological Service and Famine Early Warning System Network (FEWS NET) archives. Monthly fields were used in all instances.

3.0 Methods

Please note that in the following description we make use of the mathematical convention of using bold characters (i.e. **n**, **w**, **m**, **u**, **p**, **s**) to represent vectors, or sets of values: **n** represents a set of neighboring rain gauge observations, **w** a set of weights used to combine these observations, **m** a set of long term mean rainfall values, **s** a set of long term satellite rainfall means, and **u** a set of unbiased rainfall estimates. Individual values at some location (indexed by 'i'), are referred to as non-bold characters, so s_i indicates the long term satellite rainfall average at location i.

3.1 general formulation

A first generation rainfall estimate at a given location (e_i) is typically produced by defining a set of weights (**w**) for each location and set of neighboring stations (**n**), and then calculating the weighted sum:

$$e_i = \mathbf{n}^T \mathbf{w} \tag{1}$$

Where e_i denotes the estimate at location i, and **n** and **w** are vectors of neighboring values. $\mathbf{n}^T \mathbf{w}$ is mathematical shorthand for multiplying each n_i by the corresponding w_i and taking the sum over all locations. Typically (but not always) **w** sums to 1, and the individual weights are a function of the distance between each neighbor and location i. Second generation approaches includes estimates of a background mean.

$$e_i = (\mathbf{n} - \mathbf{m})^T \mathbf{w} + m_i \tag{2}$$

Where **m** denotes a spatially continuous mean field sampled at a set of neighboring locations. This type of estimation process takes advantage of information contained in the mean field, and interpolates anomalies from long term averages (**n-m**). The long term mean field is then added to the interpolated result (+m_i in eq. 2). This is especially useful in (the typical) cases of low gauge density, since in the absence of observations the interpolated field relaxes towards reasonable average values. Third generation approaches modify this relationship, using both time-varying satellite data (**s**) and high-resolution mean fields (**m**) to augment the interpolation process.

$$p_i = \frac{(s_i + \varepsilon)}{(\bar{s}_i + \varepsilon)}, \forall i \tag{3}$$

$$u_i = p_i m_i, \forall i \tag{4}$$

$$e_i = (\mathbf{n} - \mathbf{u})^T \mathbf{w} + u_i \tag{5}$$

The first step of this procedure (eq. 3) translates the satellite estimate at each station location s_i into a percentage, p_i, by dividing s_i by the long term mean satellite value at location I, $\bar{s}_i$. A small value (ε) is added to the numerator and denominator to force the percents to 1 as precipitation goes to zero. The $\forall i$ in eq. 3 indicates that this percentage calculation is carried out for each station. This produces a vector of at-station percentages (**p**, ranging from 0 to 1), indicating whether the satellite field is above or below 'normal'. Since satellites exhibit substantial bias, using a good long term rainfall climatology to represent the physical units of 'normality' (i.e. the typical rainfall in mm) can produce unbiased satellite estimates *without* adding any additional station data. This is achieved by multiplying each satellite percentage value p_i by that locations long term mean, m_i (eq. 4). This produces a set of unbiased satellite rainfall estimates (**u**).

Unbiased satellite values can then used to assist a standard interpolation process (eq. 5). Instead of working with differences from a long term mean (**n-m** in eq. 2), 3rd generation approaches work with differences from a long term mean, modified by satellite observations, (**n-u**). The satellite data, expressed as percentages (**p**) modulates the long term mean field. This produces estimates that benefit from the ability of satellite fields to represent *relative* differences in rainfall rates. 'Typical' rainfall amounts, however, are defined by long term mean fields.

In our implementation we actually use a two-step replacement for equation 5. In the first step the at-station ratio anomalies are interpolated. These gridded ratio fields are then multiplied against the unbiased rainfall fields, producing first guess estimates. In the second step the at-station arithmetic residuals from these estimates are calculated and interpolated. This step allows the addition of rainfall, handling the case in which satellite fields falsely record zero precipitation.

Note that equations 1-5 are quite general, and can incorporate weighting techniques derived from geo-statistics (kriging), mathematical surface fitting (splines and multiquadric formulations) and various inverse distance approaches (e.g. Cressman, Shepard, standard inverse distance weighting). Similarly the specification of the mean field or satellite data set can vary as well. Another possible permutation would be the use of distribution-specific z-score transformations rather than ratio operators. Our view is that while method choice is important, making maximum use of available data is often the quickest way to accurate precipitation estimates. In other words, many alternative data sources and specific algorithms could all produce good results, given the improved rainfall estimation (IRE) schema defined by equations 3-5.

While many choices of interpolation algorithm are available, simplicity is often required in an

operational environment. To this end we have developed a simple double-IDW (inverse distance weighting) correction tool. This tool merges stations and rainfall estimate grids in two consecutive passes. In the first pass *ratios* between stations and satellite grids are calculated and interpolated. In the second pass the ratios are multiplied against the UBRF and the arithmetic at-stations *differences* interpolated. This second pass handles instances when the UBRF is 0. The interpolated anomalies are limited by a weighting function based on the distance from the nearest neighbor. This weighting function forces the ratio and arithmetic difference fields to zero and one (respectively) as the distance from a location approaches a user-defined threshold (7° in this case). This simple approach incorporates some of the benefits of kriging, but without substantial user intervention.

3.2 The FEWS NET Climatology (FCLIM)

Orographically enhanced mean fields were produced by combining average monthly ARC grids with slope and elevation enhancement factors. The use of satellite rainfall averages as a basis for deriving improved climatologies is, as far as we know, a new innovation. This innovation grows naturally out of the fact that there are strong local regressions between station normals and monthly means ARC ($\bar{a}$). Scatter about these regression lines is in turn typically strongly related to the product of $\bar{a}$ and the local slope ($\bar{a}s$) and/or elevation ($\bar{a}e$). In other words, topography often acts to amplify a broader scale precipitation tendency, represented by $\bar{a}$, and the observed station normals ($\bar{o}$) can be reasonably fit by local regressions of the form $\bar{o} \approx b_o + b_1\bar{a} + b_2\bar{a}s + b_3\bar{a}e$. These models were fit as described in Funk and Michaelsen (2004), except that a series moving spatial windows with a 7° radius (~770 km) were used to develop localized regression models, based on weighted subsets of 6965 FAOCLIM2.0 precipitation normals (FAO, 2001). These moving window regressions produced 12 monthly 0.1° grids of average rainfall. Block kriging was then used to interpolate the 6965 at-station differences (residuals) between the FAO climate normals and regression estimate grids. The regression estimates and kriged anomalies were combined yielding 12 monthly FEWS NET climatology fields (FCLIM).

4.0 Results

4.1 FCLIM annual means.

The at-station accuracy of the FCLIM monthly long term mean fields was evaluated numerically by comparing the regression estimates at each of the 6,965 points to the modeled value for each month. The error statistics were promising, with a coefficient of determination of 0.9, a mean bias error of 0.06 mm month[-1], and mean absolute error of 18 mm month[-1]. Figure 1 shows the mean annual FCLIM precipitation and FAO climate normal locations for sub-Saharan Africa.

4.2 Ethiopia IRE Validation

A more detailed cross-validation analysis for Ethiopia examined the at-station accuracies of the full IRE process. This validation calculated at-station statistics based on 11 years (1995-2005) of CPC ARC data and 120 National Meteorological Agency (NMA) station observations. For each month during the two main rainy seasons (Belg and Meher, March-September) a 10% random sample of stations was withheld and the full IRE estimation procedure (UBRF blended with stations) executed. For each of the 77 months (11 years x 7

months) the corresponding 0.1° pixel rainfall estimates were then extracted from the ARC and IRE grids and compared to the excluded stations.

Table 1 summarizes the at-station and pooled (regional) accuracy values. At a monthly/at-station scale the mean absolute error is high (42 mm) when compared to the long term mean average monthly rainfall of 112 mm month^{-1}. The IRE bias is low (~6 mm month^{-1}), however, and averaging in space reduces this value to 18 mm month^{-1} at the monthly time scale and 8 mm month^{-1} over a season. At-station monthly, regional monthly, and regional seasonal R^2 values are reasonably high (0.62, 0.8 and 0.82 respectively). The relative error values (MAE divided by temporal standard deviation) suggest useful signal to noise ratios; 0.43, 0.34 and 0.36 for the corresponding at-station monthly, regional monthly, and regional seasonal space-time scales. Figure 2 shows time-series of the averages of the excluded stations and the associated IRE pixel estimates. The fidelity is reassuring. Figure 3 shows the monthly bias and R^2 values of ARC and IRE estimates. ARC accuracy degrades later in the season, underestimating rainfall amounts and tracking poorly with observations, perhaps due to limitations associated with the cold cloud duration threshold.

4.3 Western Kenya IRE Validation

A third detailed validation study was performed for a test site in Western Kenya (34.15°-35.55°E, 1°S-1°N). This site has been used in two previous evaluations: our accuracy assessment for the Collaborative Historical African Rainfall Model (CHARM, Funk et al., 2003) and a comparison between the CPC and NCAR-NCEP reanalysis fields (Funk and Verdin, 2003). A dense gauge network of 73 daily observations from 1961-1998 was interpolated to an 0.1° grid using inverse distance weighting. These 0.1° daily grids were accumulated to monthly totals and compared to the full IRE process driven by GPCP data.

Though coarse in resolution (2.5°) the GPCP data has the strong advantage of a climatological period of record (1979-2006, 28 years). The GPCP values were translated into ratios of the long term GPCP means and resampled using a cubic convolution to an 0.1° grid. These 0.1° ratios were multiplied against the corresponding FCLIM means, producing unbiased rainfall values. These UBRF fields were then merged with 19 stations drawn from the Global Historical Climate Network (Peterson and Vose, 1997).

The downscaled GPCP-based IRE fields recreate the long term mean structure of the region reasonably well, given the 2.5° scale of the GPCP forcing data (Figure 4). While the study site has an area equal to 45% of a GPCP grid cell, the downscaled IRE means correspond fairly well at an 0.1° resolution, with a spatial R^2 of these fields is about 0.65 (Table 2). Presumably, even better results could be achieved using higher resolution satellite observations, and more analysis along these lines needs to be carried out. As a reference, we have included regional mean absolute error and mean bias error statistics from our 2003 (Funk & Verdin, 2003) validation study based on RFE1.0 estimates (Herman et al., 1997). These values suggest that IRE based on coarse resolution GPCP data can outperform at least one traditional high-resolution satellite estimate. This is primarily due to a reduction in mean bias error.

Time-series of the monthly regional IRE averages track well with high density gauge estimates (Figure 5). These regional averages show almost no bias, and explain a

considerable proportion (87%) of the gauge variance (Table 2). Even at the 0.1° monthly scale the mean absolute error (39 mm) is only 20% of the monthly mean of 175 mm, and about 54% of the monthly temporal standard deviation. This accuracy level (½ a standard deviation) is sufficient to capture extreme hydrologic variations, but not accurate enough to guide agricultural decision making. A GPCP-driven IRE product appears like a good candidate for early warning applications. This, presumably, could be implemented globally over a 29 year period of record. Such a product could likely be a substantial improvement on '2nd generation' climatology products based just on interpolated gauge data. IRE techniques incorporated into a framework combing higher resolution satellite estimates and denser gauge networks may be accurate enough to guide farm decisions, but that remains to be evaluated.

5. Discussion
The IRE technique combines traditional rainfall interpolation approaches with satellite-based precipitation surfaces. Similar to 'smart interpolation' approaches (Willmott and Matsura, 1995) commonly used to produce gridded fields (New et al. 1999, 2000), the IRE procedure is assisted by a long term mean field. In addition to these mean fields, the IRE is also assisted by time-varying satellite rainfall estimates. The recent decline in readily available high quality gauge data makes the use of satellite data critical, especially in many climatically and environmentally important areas of the developing world. Many of the complexities associated with orographic precipitation modeling at monthly and seasonal scales can be absorbed within sophisticated, topographically enhanced mean precipitation grids. These background fields can be used to remove the systematic bias commonly found in satellite precipitation fields, producing unbiased rainfall estimates (UBRF). This procedure can also be used to introduce local variations into coarse precipitation surfaces, such as those produced by the 2.5° Global Precipitation Climatology Project (GPCP, Huffman et al., 1995, 1997, Adler et al., 2003). The unbiased satellite estimates, in turn, can in turn be combined with station data in a geostatistical framework (an idea originally inspired by Grimes et al., 1999) with the final product referred to in this paper as improved rainfall estimates (IRE). Note that 'improved' does not imply that the original satellite estimates are 'bad', but rather that additional information has been added.

The improved rainfall estimation procedure has three distinct steps: i) the creation of satellite-enhanced long term mean fields (FCLIM), ii) the combination of the these fields with time-varying satellite fields to produce unbiased time-varying estimates (UBRF), and the iii) fusion of these time-varying satellite estimates with regional near-real time station data (IRE). The objective is to use all available sources of data to produce accurate, low bias, consistent rainfall fields in a moderately timely manner.

In Africa, effective rainfall estimates (RFE) form the basis of hydrologic early warning. Effectiveness may be defined along several dimensions, with accuracy, low bias, consistency, and timeliness forming a minimal set. Accuracy refers to an RFE's capacity to recreate the space-time covariance of 'true' rainfall, typically defined by high quality station data. Consistency is a related criterion that establishes reasonably station distribution parameters over a climatological period of record. The explicit meaning of 'timeliness' varies with application. We focus here on a monthly 'hydro-climatic' time-scale, and assume that a timely estimate may be prepared with a one or two week lag. At present, FEWS NET uses multi-satellite RFE2.0 (Xie and Arkin, 1997) and the longer single-satellite African Rainfall

Climatology (ARC, Love et al., 2004). Both sets of estimates are constrained by Global Telecommunication System (GTS) observations. These excellent data sets are timely and reasonably accurate, and the 11 year ARC provides a reasonable basis for estimating rainfall means (a first order statistic).

Unfortunately, the GTS network is quite sparse and many additional stations are typically available to National Meteorological Agencies. The RFE2.0 and ARC also tend to exhibit substantial bias at certain seasons and locations (Funk, 2002; Funk & Verdin 2003). This is especially true in complex terrain. After several years spent working with internal gravity waves as a basis for orographic enhancement (Funk et al., 2003; Funk and Michaelsen, 2004), we believe that sophisticated monthly mean fields can be used in near real time to parsimoniously remove substantial bias from satellite RFE, producing unbiased rainfall estimates (UBRF). These UBRF grids may then be augmented by dense non-GTS station observations to produce Improved Rainfall Estimates (IRE).

References
Adler, R.F., G.J. Huffman, A. Chang, R. Ferraro, P. Xie, J. Janowiak, B. Rudolf, U. Schneider, S. Curtis, D. Bolvin, A. Gruber, J. Susskind, and P. Arkin, 2003: The Version 2 Global Precipitation Climatology Project (GPCP) Monthly Precipitation Analysis (1979-Present). J. Hydrometeor., 4,1147-1167.

FAO Agrometeorology Group. 2001: FAOCLIM 2.01 Worldwide Agroclimatic Database [CD-ROM]. Food and Agricultural Organization of the United Nations (FAO), Rome.

Funk, C., 2002: Operational Assessments of Satellite RFE Accuracy; USGS Internal FEWS NET Report, November 2002.

Funk, C., J. Michaelsen, J. Verdin, G. Artan, G. Husak, G. Senay, H. Gadain, and T. Magadazire, 2003a: The Collaborative Historical African Rainfall Model: Description and Evaluation. International Journal of Climatology, 23, 47-66

Funk, C.; T. Magadzire, G. Husak, 2003: Crop Production Outlook for Southern Africa. FEWS NEW Special Report, December 2003.

Funk, C. and J. Verdin, 2003: Comparing Satellite Rainfall Estimates and Reanalysis Precipitation Fields with Station Data for Western Kenya. International workshop on crop monitoring and early warning for food security, Nairobi, JRC - FAO. January 28th -30th, 2003.

Funk, C. and J. Michaelsen, 2004: A simplified diagnostic model of orographic rainfall for enhancing satellite-based rainfall estimates in data poor regions. Journal of Applied Meteorology, V34. 1366-1378

Gesch, D.B., K.L. Verdin and S.K. Greenlee, 1999: New land surface digital elevation model covers the Earth. EOS, Transactions of the American Geophysical Union, v. 80, n. 6, pp. 69-70.

Herman, A., Kumar V. B., Arkin P. A. and Kousky, J. V. 1997: "Objectively determined 10-day African rainfall estimates created for famine early warning systems", Int. J. Remote Sensing, 18(10) 2147-2159.

Huffman, G.J., R.F. Adler, B. Rudolph, U. Schneider, and P. Keehn, 1995: "Global Precipitation Estimates Based on a Technique for Combining Satellite-Based Estimates, Rain Gauge Analysis, and NWP Model Precipitation Information", J. Clim., 8, 1284-1295.

Huffman, G.J., R.F. Adler, P. Arkin, A. Chang, R. Ferraro, A. Gruber, J. Janowiak, A. McNab, B. Rudolph, and U. Schneider, 1997: "The Global Precipitation Climatology Project (GPCP) Combined Precipitation Dataset", Bul. Amer. Meteor. Soc., 78, 5-20.

Love, T., V. Kumar, P. Xie and W. Thiaw, 2004: A 20-year daily Africa precipitation climatology using satellite and gauge data, American Meteorology Society Conference on Applied Climatology. P5.4, Wednesday, Jan 14th, 2004. Seattle, Washington.

New, M., M. Hulme, P. Jones, 1999: Representing twentieth-century space-time climate variability. I. Development of a 1961-90 mean monthly terrestrial climatology. Journal of Climate, 12(3): 829-56.

New, M., M. Hulme, M. and P. Jones, 2000: Representing twentieth-century space-time climate variability. II. Development of 1901-96 monthly grids of terrestrial surface climate. Journal of Climate, 13(13): 2217-38.

Peterson, T.C. and R.S. Vose, 1997: An overview of the Global Historical Climatology Network temperature data base. Bulletin of the American Meteorological Society, 78: 2837-2849.

Willmott, C.J. and K. Matsura, 1995: Smart Interpolation of Annually Averaged Air Temperature in the United States. Journal of Applied Meteorology, 34: 2577-2586.

Xie, P. and P.A. Arkin, 1997: Global Precipitation: A 17-Year Monthly Analysis Based on Gauge Observations, Satellite Estimates and Numerical Model Outputs. Bulletin of the American Meteorological Society, 78(11): 2539-2558.

Tables

Table 1. Ethiopian test site evaluation statistics. The March-September and Monthly rows report statistics for the seasonal March-September and individual monthly March-September accumulations, respectively. The first and second columns report mean bias and mean absolute errors based on the average of all stations. The MAE STD^{-1} column provides a relative metric of uncertainty, with typical errors being about ~33% of the temporal standard deviation. The time R^2 is calculated using 11 years of data (1995-2005). The last three columns are similar to the regional metrics, but based on calculations using the individual station values. Seasonal at-station values were not available do to the random sampling associated with the cross-validation.

IRE	Regional Metrics				At-station metrics		
	MBE	MAE	MAE STD^{-1}	Time R^2	MAE	MAE STD^{-1}	Time R^2
Seasonal	6	8	0.36	0.82	---	---	---
Monthly	6	18	0.34	0.80	42	0.43	0.62

Table 2. Kenya test site evaluation statistics. The MAM and Monthly rows report statistics for the seasonal March-May and individual March-April-May accumulations, respectively. The first column reports the R^2 of the long term (1979-2005) averages at the 294 (14 rows x 21 columns) 0.1° pixels. The second and third columns report mean bias and mean absolute errors based on the average of all 294 pixels. MAE and MBE are reported in mm month^{-1}. The MAE STD^{-1} column provides a relative metric of uncertainty, with typical errors being about ~33% of the temporal standard deviation. The time R^2 is calculated using 27 years of data (1979-2005). The last three columns are similar to the regional metrics, but based on calculations using the individual 0.1° values.

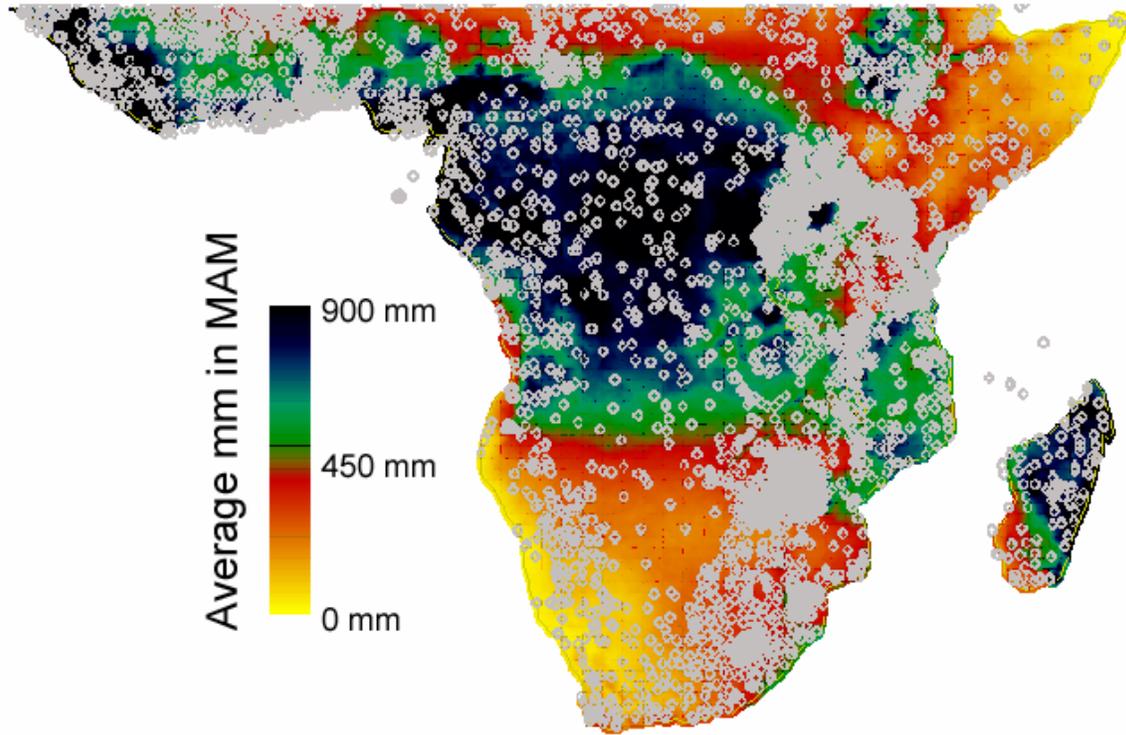|	Regional Metrics					At-pixel metrics		
	Spatial R^2	MBE	MAE	MAE STD^{-1}	Time R^2	MAE	MAE STD^{-1}	Time R^2
Seasonal	0.67	0.01	8	0.31	0.87	26	0.52	0.54
Monthly	0.64	0.00	14	0.37	0.75	39	0.54	0.49
Monthly RFE1.0		15	20					

Figures

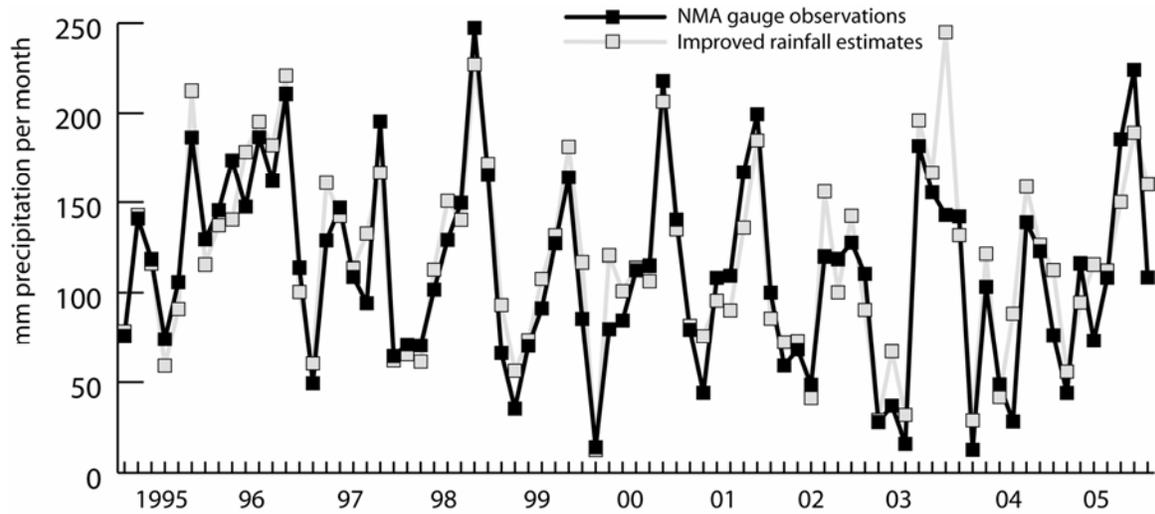Figure 1. FCLIM annual means and FA0CLIM 2.0 station locations for sub-Saharan Africa.

Figure 2. Ethiopian observed and cross-validated monthly averages. Each observed datum is based on the average of a 10% sample of the NMA gauge network. The corresponding 0.1° IRE pixels were also averaged and plotted. The seven months of the main growing seasons (March-September) are shown.
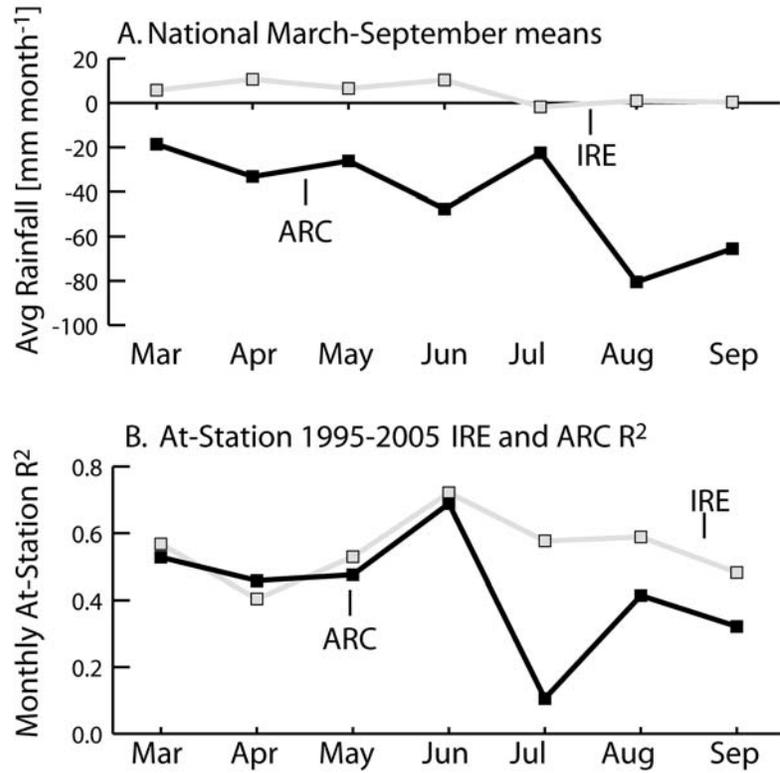
Figure 3. Monthly rainfall bias and R^2 values for the Ethiopian test site.
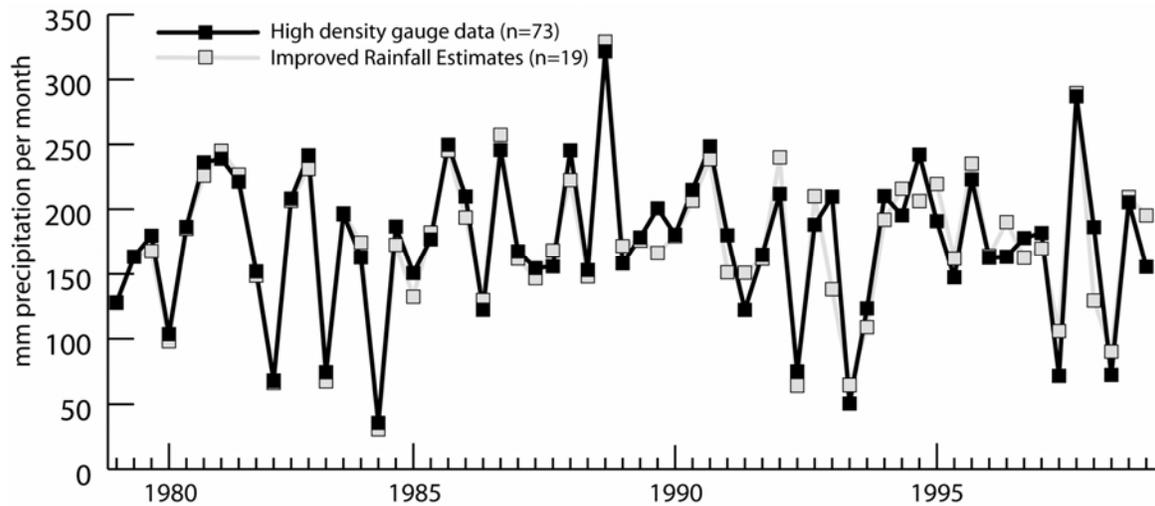

Figure 4. Regionally averaged 1979-1998 March-April-May rainfall over the western Kenya test site. The first three boxes represents three month from 1979(March, April and May). Each consecutive set of three boxes represents one of the following years.
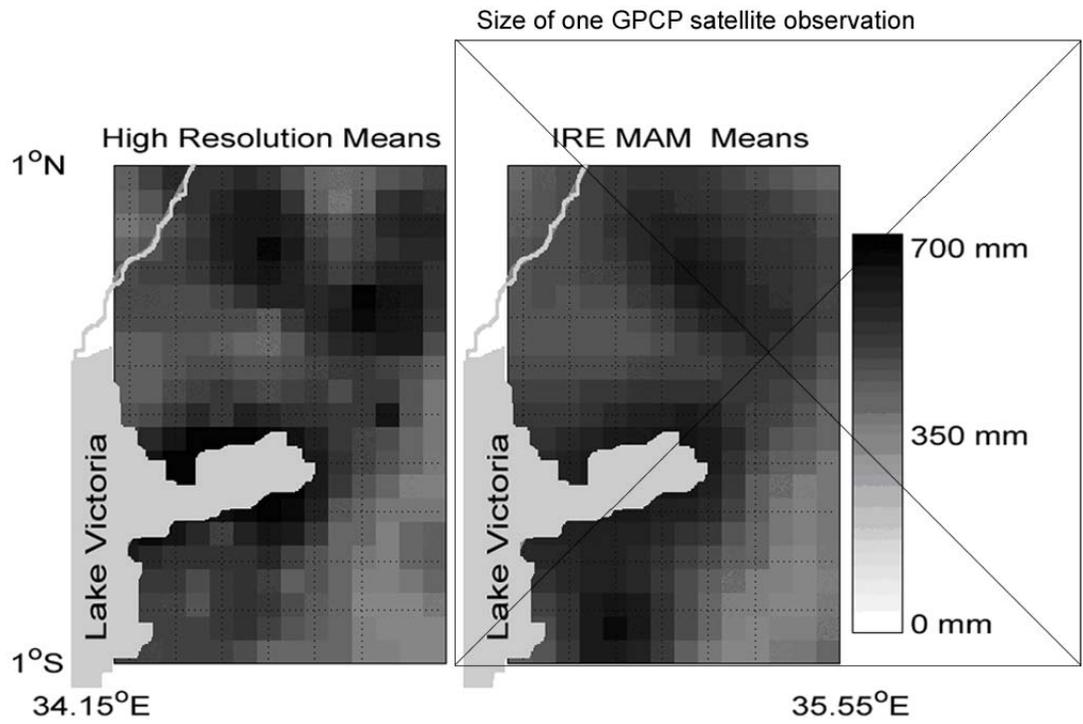
Figure 5. Monthly March-April-May mean 1979-1998 high density gauge and improved rainfall estimates over the Kenya test site.